

## ***Ab Initio* Photoabsorption Spectra and Structures of Small Semiconductor and Metal Clusters**

Angel Rubio,<sup>1,2</sup> J. A. Alonso,<sup>1</sup> X. Blase,<sup>2,\*</sup> L. C. Balbás,<sup>1</sup> and Steven G. Louie<sup>2</sup>

<sup>1</sup>*Departamento Física Teórica, Universidad de Valladolid, E-47011 Valladolid, Spain*

<sup>2</sup>*Department of Physics, University of California at Berkeley, Berkeley, California 94720  
and Materials Sciences Division, Lawrence Berkeley National Laboratory, Berkeley, California 94720*

(Received 16 April 1996)

*Ab initio* photoabsorption cross sections of small silicon and alkali clusters (Li, Na) have been calculated by a new method. Different structural isomers of a given silicon cluster give rise to clearly distinguishable spectra. Inclusion of screening effects is shown to be essential to describe the spectra. We propose that comparison of theoretical spectra with measured ones would serve as a useful tool to discern the structure of small semiconductor clusters. Low temperature measurements and/or line-shape analysis are needed to extract detailed structural information from the spectra of alkali clusters because of the collective character of the main resonance. [S0031-9007(96)00571-6]

PACS numbers: 36.40.Mr, 31.15.Ar

The interplay between the electronic degrees of freedom and the geometrical structure in small atomic aggregates has attracted a lot of interest [1,2]. The determination of the geometry of clusters is central for a deeper understanding of their electronic, chemical, and magnetic properties. Both metal and semiconductor clusters undergo substantial structural reconstruction as they grow, which affects their chemical reactivity, photofragmentation, and Raman and photoelectron spectra [3–5], but no systematic method allowing for extraction of the geometry from experiment is available yet.

The measured multiphoton absorption spectra of medium size silicon clusters ( $\text{Si}_N$ ,  $18 \leq N \leq 41$ ) show similarities with the spectrum of bulk crystalline silicon [6]. This indicates that Si clusters formed by tens of atoms have already developed a common basic structural entity. However, for small sizes, the photoelectron spectra seem to mirror the changes in geometrical structure [5,7]. Raman spectroscopy has been used for the identification of isomers in small silicon clusters [4], arriving at structures showing good agreement with those predicted by theoretical calculations [7]. In a recent theoretical analysis of the ultraviolet spectra of small silicon cluster anions, Binggeli and Chelikowsky [8] have shown the importance of structural relaxation of the charged cluster with respect to the neutral one. By comparing the density of electronic states of different isomers obtained in a density-functional (LDA) calculation with the measured photoemission spectra [5], Binggeli and Chelikowsky were able to identify the relevant isomers. In the present paper, we perform linear response calculations within the time-dependent local density-functional formalism (TDLDA) [9], and we show that a simple consideration of particle-hole excitations, as reflected in the single-particle density of states, is not enough to describe in detail the photoabsorption spectra of small silicon clusters; that is, electron screening and final state effects play a significant role.

This is even more evident in the case of metallic clusters [10]. In contrast to semiconductors, the photoabsorption

spectra of alkali metal clusters like  $\text{Na}_N$  or  $\text{K}_N$  is dominated by a collective resonance (surface plasmon) that can be described by the classical Mie dipole oscillation, whose frequency is given by  $\omega^2 = e^2 N / m R^3$ , where  $e$  and  $m$  are the electron charge and mass, respectively,  $N$  is the number of conduction electrons in the droplet, and  $R$  the droplet radius. However, the observed resonance is shifted to lower frequencies, and the magnitude of this shift is semi-quantitatively reproduced by the TDLDA within the framework of the spherical jellium (homogeneous background) model [2]. In some small clusters, the plasmon line is split into two or three components, reflecting the deviation of the overall cluster shape from spherical symmetry. This splitting is also explained by allowing for ellipsoidal or more complex shape deformations in the jellium model [2,11]. But, for Li clusters, the shift of the plasmon line and its broadening are larger than in Na and K clusters [12]. An explanation of these effects cannot be achieved within the context of the jellium model since they are related to the ionic contributions to the electronic effective mass. Although no direct information about cluster geometries has been extracted from the Li experiments, *ab initio* molecular dynamics simulations have provided predictions of the packing and growth of small and medium size Li clusters [13].

Thermal broadening of the optical spectra reflects an important coupling to vibrations in both metallic [14] and semiconductor clusters [6]. This has been studied in detail by Ellert *et al.* [14]. The spectra of small sodium clusters at temperatures higher than 350 K can be explained by considering the cluster as a soft homogeneous droplet, not necessarily spherical. However, the low temperature spectra contains sharp molecularlike features that should reveal the detailed geometric structure of the cold cluster [15].

In this Letter, we focus on the ability to extract detailed geometrical information by a comparison of the measured photoabsorption spectra and the polarizabilities of small Li [1,16] and Si clusters [6,17] with the TDLDA spectra

of several low energy isomers (for a given cluster size) calculated by a new method to compute the dielectric response, including local-field and screening effects, developed recently by some of us [18]. The dielectric response, as obtained in linear response theory, is not only a key ingredient to explain the optical spectra but also an important ingredient in the description of quasiparticle excitations within a perturbation expansion of the self-energy operator in the *GW* method [19]. The *GW* approximation has been successfully used by Onida *et al.* [20] to include excitonic effects in the absorption spectrum of  $\text{Na}_4$ . Dynamical screening significantly affects the static and dynamical response of atoms, molecules, and solids to an external electromagnetic field. Compared to independent-particle calculations, the linear and nonlinear polarizabilities are reduced [1,21]. For large frequencies (as probed in photoemission experiments) the collective effects tend to shift oscillator strength to higher frequencies, and, in the case of metallic clusters, several particle-hole transitions often lose their individual identity and merge into a broadened collective resonance [9].

The *ab initio* density-functional pseudopotential scheme has been combined with a conjugate-gradient method to obtain the geometry that minimizes the ground-state energy of the cluster. The LDA was used for exchange and correlation effects [22]. The clusters are described using a periodic fcc supercell of edge  $a = 36$  a.u. Norm-conserving pseudopotentials have been generated as proposed in Ref. [23], and a plane-wave energy cutoff of 10 Ry was used. Convergence in both energy cutoff and cell size has been carefully tested. The theory for the response to an external field within the TDLDA has been described elsewhere [9,18]. The main ingredient is the computation of the dielectric function  $\epsilon(\vec{r}_1, \vec{r}_2, \omega)$  in a spatial grid. We take advantage of the short range of the dielectric function, and for each point  $\vec{r}_1$  we consider points  $\vec{r}_2$  within a localization sphere of radius 9.5 Å; in this way the number of pairs  $(\vec{r}_1, \vec{r}_2)$  where  $\epsilon(\vec{r}_1, \vec{r}_2, \omega)$  needs to be evaluated is reduced significantly. The combination of this localization range with an imaginary-time technique for the dynamical calculation leads to a  $N^2$  scaling of the method [18]. In the present work  $\epsilon(\vec{r}_1, \vec{r}_2, \omega)$  is computed by summation over occupied and unoccupied bands by including 60 bands per atom; this gives a good convergence in the range of frequencies under study. Once the ground-state wave functions have been computed, they are fast-Fourier transformed to a real-space mesh and truncated for points outside the unit cell [24]. This allows us to perform all the response calculations in real space. The scheme (see Ref. [18] for details) is faster than traditional Fourier-space calculations. Although single-particle excitations are not well described as differences of LDA eigenvalues, Petersilka *et al.* [25] have proved that time-dependent density-functional theory allows the calculation of excitation energies. Thus we expect that the present absorption spectra would reproduce the main features of the experimental one, besides excitonic effects.

As a first test case of the new response method, we consider  $\text{Li}_8$  because accurate photoabsorption cross sections have been measured for this cluster which do not fit into the free-electron picture [16]. Our calculated ground-state geometry, shown in the inset of Fig. 1, is a centered trigonal prism with an atom capping one of the rectangular faces, in agreement with that obtained by Sung, Kawai, and Weare [13]. The average bond length is 2.7 Å, and the radius of an equivalent sphere with the same volume of the cluster is  $R = 2.4$  Å. Classically the polarizability of a spherical metallic droplet of radius  $R$  is proportional to  $R^3$ . Some quantum effects can be included by measuring the droplet radius by  $R + \delta$ , where  $\delta = 0.8$  Å represents the electronic spillout [2,21]. Then we estimate a polarizability  $\alpha = 32$  Å<sup>3</sup>. Our *ab initio* averaged value  $\frac{1}{3}(\alpha_{xx} + \alpha_{yy} + \alpha_{zz})$  gives 33 Å<sup>3</sup>, and a linear response calculation within the spherical jellium model gives  $\alpha = 63$  Å<sup>3</sup>. The large discrepancy between the two linear response calculations is due to the compression of the bond length with respect to the bulk value, a usual effect in metallic clusters [21] which is not included in the jellium model.

In the classical Mie theory, the lower the polarizability the larger the collective resonance frequency. Then a blueshift of the resonance frequency with respect to the jellium value of 3.5 eV should be expected; instead, a redshift of 1 eV is observed in the experiment [16]. In Fig. 1 the *ab initio* averaged photoabsorption cross section is compared to the independent-particle and jellium model cross sections. A broadening of 0.1 eV was used to simulate

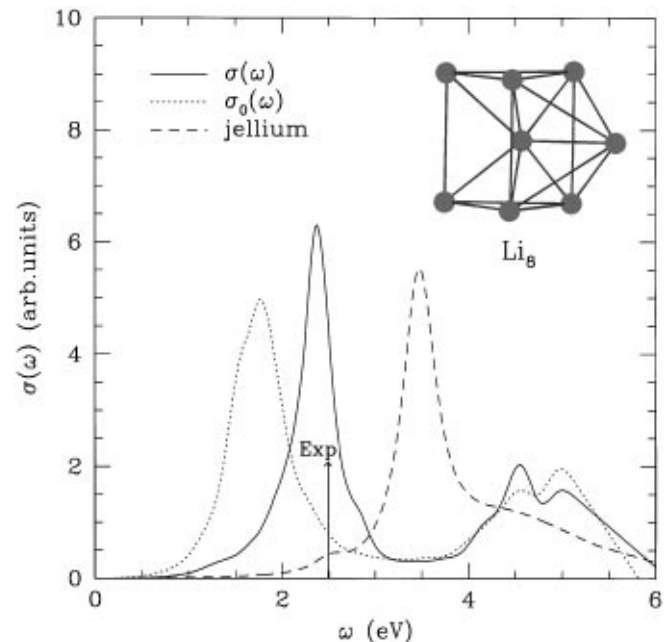


FIG. 1. Averaged TDLDA photoabsorption cross section for  $\text{Li}_8$  obtained in *ab initio* and jellium calculations. The continuous and dotted curves correspond to the fully interacting and independent-particle response, respectively. The experimental resonance frequency of 2.5 eV is indicated by the vertical arrow. The inset shows the ground-state geometry from total energy minimization.

temperature effects. The nearly isotropic polarizability tensor explains the presence of a unique resonance at 2.45 eV in the *ab initio* spectrum, in very good agreement with the experimental value of 2.5 eV [16]. The redshift with respect to the jellium frequency is due to an increase of the electronic effective mass  $m^*$ , since  $\omega^2 = e^2 N / m^* \alpha$ . The arguments given above lead to  $m^* \sim 1.4m$ , much larger than for other alkali clusters and in agreement with the experimental observations for planar surfaces and large Li clusters [12]. A new feature predicted by the present calculation is a broad hump in the absorption spectra for frequencies above 4 eV that is connected with the onset of the LDA ionization threshold (4 eV) and which consists of mainly particle-hole transitions already present in the independent-particle absorption cross section. Experiments could observe this new structure in the spectrum that is absent in other alkali clusters of similar size.

We briefly comment on the results for  $\text{Na}_8$ . The ground-state structure (bicapped octahedron;  $D_{2d}$  symmetry) leads to a polarizability tensor with two different components ( $\alpha = 115$  and  $125 \text{ \AA}^3$ ) and two close-lying peaks are obtained in the photoabsorption cross section. The averaged polarizability of  $119 \text{ \AA}^3$  is in good agreement with the experimental value of  $123 \text{ \AA}^3$  [1]. Once a broadening of the resonances is introduced we obtain a main peak centered at 2.55 eV [26] (the experimental value is 2.53 eV [1] and the spherical jellium value is 2.9 eV [21]). The compact tetrahedral structure of an isomer with  $T_d$  symmetry (tetracapped tetrahedron) [15] leads to an isotropic polarizability tensor and a single resonance peak. Consequently, low temperature measurements and line-shape analysis are needed to distinguish between the two isomers. On the other hand, a comparison of the interacting and single-particle cross sections shows that inclusion of exchange-correlation effects in the dielectric response is required to get the correct resonance frequency.

As a second class of systems, we apply our approach to silicon clusters. Raman spectroscopy has allowed the identification of the geometry of  $\text{Si}_4$  and  $\text{Si}_6$  [4], and *ab initio* calculations of their structure have also been performed [7,8]. The ground-state geometry that we have obtained for  $\text{Si}_4$  is a planar rhombus ( $D_{2h}$ ). This is shown in Fig. 2 together with a tetrahedral isomer ( $T_d$ ) 1.7 eV above in energy. Two nearly isoenergetic structures are predicted for  $\text{Si}_6$ : a distorted octahedron ( $D_{4h}$ ) and an edge-capped trigonal bipyramid ( $C_{2v}$ ), the first one slightly more stable (0.02 eV). The distortion of the octahedron (2.4/2.7 is the ratio of bond lengths shown in Fig. 2) is slightly smaller than the distortion (2.54/2.93) given in Ref. [7]. This will increase a little the  $B_{2g}$  and decrease the  $E_g$  Raman active modes, improving the agreement with the experiment [4]. Our minimum energy structures coincide with those experimentally identified.

Figure 2 shows that one can extract isomeric information from the photoabsorption spectra. The calculated single photon averaged absorption profiles have been plot-

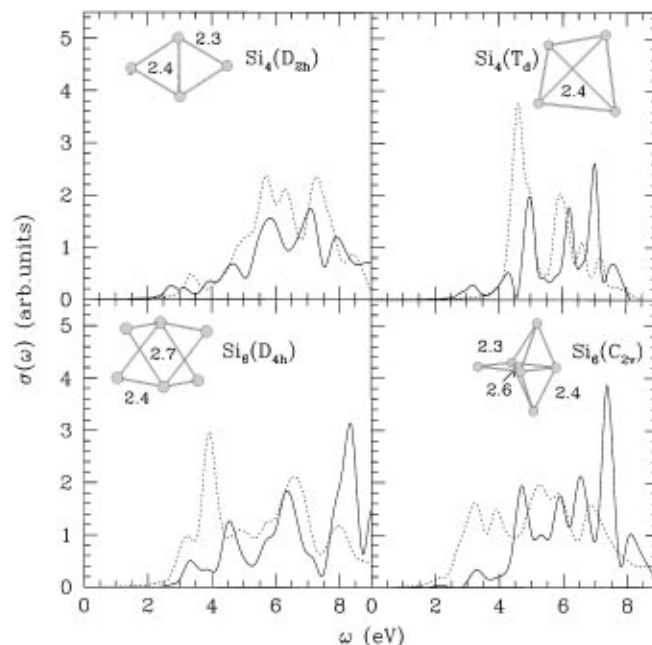


FIG. 2. The averaged photoabsorption cross sections of  $\text{Si}_4$  and  $\text{Si}_6$  for the geometries shown in the insets. The continuous and dotted curves correspond to the fully interacting and independent-particle response, respectively.

ted for the isomers discussed above. All the spectra have been broadened by 0.1 eV to simulate finite temperature. As a general trend we predict a broad structure starting around 3 eV that agrees with the features seen in the measured multiphoton absorption spectra for larger clusters [6]. More important, different isomers of the same cluster lead to very different photoabsorption cross sections. Even more striking differences are obtained for each tensor component of the absorption cross section. In  $\text{Si}_4$  the absorption tensor is isotropic for the three-dimensional  $T_d$  structure, whereas for the planar  $D_{2d}$  structure it shows a strong reduction of the absorption in the perpendicular direction to the plane. Comparing the independent-particle spectra to the fully interacting ones shows that electron-electron interactions induce a blueshift (more pronounced in  $\text{Si}_6$ ) and an important redistribution of the oscillator strength. The effect is smaller than in metallic clusters but still important to have a correct description of the peak positions and intensities seen in photoemission experiments as compared to the simpler density of states arguments used before [8]. The finite-size quantum-confinement effects are responsible for the appearance of absorption in the optical range and the onset of absorption is due to plasmonlike resonances (as obtained in a jellium model). This shows that small clusters can present different optical properties compared to the bulk material.

Recent measurements [17] of the static polarizability of  $\text{Si}_N$  ( $N \geq 8$ ) indicate a pronounced oscillation with cluster size and that for large clusters ( $60 < N < 120$ ) the polarizabilities reach values below the bulk limit of  $3.71 \text{ \AA}^3$  per atom. The last feature contrasts with the case

of metallic clusters, for which the bulk limit is reached from above. This shows that collective effects, which are dominant in metallic clusters, are less relevant in semiconductor clusters, in which screened particle-hole-like excitations are much more important (the same conclusion has been reached above in the discussion of the absorption spectra). We have calculated the averaged polarizabilities of  $\text{Si}_4$  and  $\text{Si}_6$ . In the former cluster the polarizability (per atom) of the two dimensional  $D_{2h}$  isomer is  $3.3 \text{ \AA}^3$ , and it drastically drops to  $2.3 \text{ \AA}^3$  for the three dimensional  $T_d$  structure. The difference between the  $D_{4h}$  and  $C_{2v}$  isomers of  $\text{Si}_6$  is smaller; these have polarizabilities of  $3.7$  and  $4.2 \text{ \AA}^3$ , respectively. All these numbers fit well within the range of the experimental values. Therefore, a combination of static and dynamical measurements with the corresponding theoretical calculations could provide valuable information on the structure of small aggregates. Average values are accessible to many experimental setups, but an analysis of the absorption tensor using polarized light in an oriented cluster beam should provide more detailed information.

In conclusion, we have applied a new method for the dielectric screening in finite systems to small silicon and alkali clusters. The method can easily be extended to larger clusters, and it constitutes the basis for modern quasiparticle calculations. We have demonstrated that a comparison of experimental and theoretical photoabsorption spectra can be used as a tool to get information on the structural properties of small semiconductor and metallic clusters. Finite-size effects introduce new peaks in the visible range for Si clusters, and screening effects are important for a correct description of the spectra. In the case of Li clusters, the correct description of the electron-ion interaction is crucial to explain the anomalous redshift of the collective resonance with respect to the jellium value. Other alkali metal clusters are also well described within the present scheme: the electron-ion interaction together with a microscopic description of the geometry of the cluster reduces systematically the errors for the polarizabilities and plasma frequencies.

This work was supported by JCL (Grant No. VA25/95), DGYCIT (Grant No. PB92-0645), CESCO, NSF (Grant No. DMR-9520554) and DOE (Contract No. DE-AC03-76SF00098). S. G. L. acknowledges the support of the Miller Institute for Basic Research in Science.

---

\*Present address: Institut Romand de Recherche Numérique en Physique des Matériaux (IRRMA), IN

- Ecublens, 1015 Lausanne, Switzerland.
- [1] W. A. de Heer, *Rev. Mod. Phys.* **65**, 611 (1993).
  - [2] M. Brack, *Rev. Mod. Phys.* **65**, 677 (1993).
  - [3] M. F. Jarrold, *Science* **252**, 1085 (1991).
  - [4] E. C. Honea *et al.*, *Nature (London)* **366**, 42 (1993).
  - [5] O. Cheshnovsky *et al.*, *Chem. Phys. Lett.* **138**, 119 (1987).
  - [6] K. D. Rinnen and M. L. Mandich, *Phys. Rev. Lett.* **69**, 1823 (1992).
  - [7] K. Raghavachari, *J. Chem. Phys.* **84**, 5672 (1986); *Phys. Rev. Lett.* **55**, 2853 (1985); X. D. Jing, N. Troullier, and J. R. Chelikowsky, *Solid State Commun.* **96**, 231 (1995).
  - [8] N. Binggeli and J. R. Chelikowsky, *Phys. Rev. Lett.* **75**, 493 (1995).
  - [9] A. Zangwill and P. Soven, *Phys. Rev. A* **21**, 1561 (1980); E. K. U. Gross and W. Kohn, *Phys. Rev. Lett.* **55**, 2850 (1985); **57**, 923(E) (1986).
  - [10] C. Massobrio, A. Pasquarello, and R. Car, *Phys. Rev. Lett.* **75**, 2104 (1995).
  - [11] S. Kasperl, C. Kohl, and P. G. Reinhard, *Phys. Lett. A* **206**, 21 (1995).
  - [12] C. Bréchnignac *et al.*, *Phys. Rev. Lett.* **70**, 2036 (1993).
  - [13] M. W. Sung, R. Kawai, and J. H. Weare, *Phys. Rev. Lett.* **73**, 3552 (1994).
  - [14] C. Ellert *et al.*, *Phys. Rev. Lett.* **75**, 1731 (1995).
  - [15] V. Bonacic-Koutecky *et al.*, *J. Chem. Phys.* **104**, 1427 (1996).
  - [16] J. Blanc *et al.*, *J. Chem. Phys.* **96**, 1793 (1992).
  - [17] R. Schäfer *et al.*, *Phys. Rev. Lett.* **76**, 471 (1996).
  - [18] X. Blase, A. Rubio, S. G. Louie, and M. L. Cohen, *Phys. Rev. B* **52**, R2225 (1995); (to be published).
  - [19] L. Hedin, *Phys. Rev.* **139**, 796 (1965); M. S. Hybertsen and S. G. Louie, *Phys. Rev. Lett.* **55**, 1418 (1985); *Phys. Rev. B* **34**, 6656 (1986).
  - [20] G. Onida *et al.*, *Phys. Rev. Lett.* **75**, 818 (1995).
  - [21] A. Rubio, L. C. Balbás, and J. A. Alonso, *Z. Phys. D* **19**, 93 (1991); *Phys. Rev. B* **45**, 13 657 (1992).
  - [22] D. M. Ceperley and B. J. Alder, *Phys. Rev. Lett.* **45**, 1196 (1980); J. P. Perdew and A. Zunger, *Phys. Rev. B* **23**, 5048 (1981).
  - [23] N. Troullier and J. L. Martins, *Phys. Rev. B* **43**, 1993 (1991).
  - [24] The minimum spatial grid ( $10 \times 10 \times 10$  for  $\text{Si}_4$  and  $12 \times 12 \times 12$  for other clusters) has been chosen in such a way that the charge density, wave functions, and orthogonality are fulfilled better than  $10^{-5}$ . Thus the matrix elements of  $\epsilon(\vec{r}_1, \vec{r}_2, \omega)$  are expected to be very accurate.
  - [25] M. Petersilka, U. J. Gossmann, and E. K. U. Gross, *Phys. Rev. Lett.* **76**, 1212 (1996).
  - [26] A. Rubio, J. M. Pacheco, and J. L. Martins (unpublished).